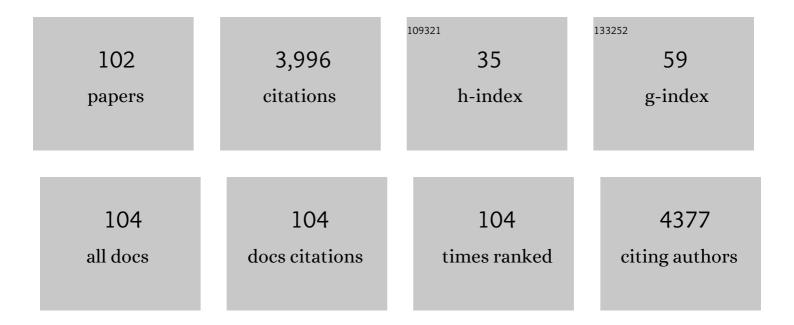
Linxi Hou

List of Publications by Year in descending order

Source: https://exaly.com/author-pdf/6205668/publications.pdf Version: 2024-02-01



#	Article	IF	CITATIONS
1	Highly tough supramolecular double network hydrogel electrolytes for an artificial flexible and low-temperature tolerant sensor. Journal of Materials Chemistry A, 2020, 8, 6776-6784.	10.3	220
2	Self-powered integrated system of a strain sensor and flexible all-solid-state supercapacitor by using a high performance ionic organohydrogel. Materials Horizons, 2020, 7, 2085-2096.	12.2	187
3	Hierarchical Porous Co ₉ S ₈ /Nitrogen-Doped Carbon@MoS ₂ Polyhedrons as pH Universal Electrocatalysts for Highly Efficient Hydrogen Evolution Reaction. ACS Applied Materials & Interfaces, 2017, 9, 28394-28405.	8.0	179
4	Template synthesis of CoSe ₂ /Co ₃ Se ₄ nanotubes: tuning of their crystal structures for photovoltaics and hydrogen evolution in alkaline medium. Journal of Materials Chemistry A, 2017, 5, 4513-4526.	10.3	165
5	A mussel-inspired supramolecular hydrogel with robust tissue anchor for rapid hemostasis of arterial and visceral bleedings. Bioactive Materials, 2021, 6, 2829-2840.	15.6	152
6	Multifunctional Poly(vinyl alcohol) Nanocomposite Organohydrogel for Flexible Strain and Temperature Sensor. ACS Applied Materials & Interfaces, 2020, 12, 40815-40827.	8.0	141
7	Preparation and characterization of poly(vinyl alcohol)/sodium alginate hydrogel with high toughness and electric conductivity. Carbohydrate Polymers, 2018, 186, 377-383.	10.2	135
8	Morphology-Tuned Synthesis of Nickel Cobalt Selenides as Highly Efficient Pt-Free Counter Electrode Catalysts for Dye-Sensitized Solar Cells. ACS Applied Materials & Interfaces, 2016, 8, 29486-29495.	8.0	117
9	Metal-organic framework-derived Ni–Co alloy@carbon microspheres as high-performance counter electrode catalysts for dye-sensitized solar cells. Chemical Engineering Journal, 2018, 334, 419-431.	12.7	111
10	Stimuliâ€Responsive Nanoparticles for Controlled Drug Delivery in Synergistic Cancer Immunotherapy. Advanced Science, 2022, 9, e2103444.	11.2	102
11	Highly tough, freezing-tolerant, healable and thermoplastic starch/poly(vinyl alcohol) organohydrogels for flexible electronic devices. Journal of Materials Chemistry A, 2021, 9, 18406-18420.	10.3	91
12	Low-cost and highly efficient CoMoS4/NiMoS4-based electrocatalysts for hydrogen evolution reactions over a wide pH range. Electrochimica Acta, 2016, 213, 236-243.	5.2	82
13	Nickel Cobalt Sulfide Double-Shelled Hollow Nanospheres as Superior Bifunctional Electrocatalysts for Photovoltaics and Alkaline Hydrogen Evolution. ACS Applied Materials & Interfaces, 2018, 10, 9379-9389.	8.0	80
14	Indolo[3,2-b]carbazole-based multi-donor–π–acceptor type organic dyes for highly efficient dye-sensitized solar cells. Journal of Power Sources, 2016, 319, 39-47.	7.8	76
15	NiCo-Layered Double Hydroxide-Derived B-Doped CoP/Ni ₂ P Hollow Nanoprisms as High-Efficiency Electrocatalysts for Hydrogen Evolution Reaction. ACS Applied Materials & Interfaces, 2021, 13, 9932-9941.	8.0	72
16	Shape-controllable syntheses of ternary Ni-Co-Se alloy hollow microspheres as highly efficient catalytic materials for dye-sensitized solar cells. Chemical Engineering Journal, 2017, 315, 562-572.	12.7	69
17	Co-Fe-MoS hollow nanoboxes as high-performance counter electrode catalysts for Pt-free dye-sensitized solar cells. Chemical Engineering Journal, 2018, 343, 86-94.	12.7	68
18	High-performance and flexible solid-state supercapacitors based on high toughness and thermoplastic poly(vinyl alcohol)/NaCl/glycerol supramolecular gel polymer electrolyte. Electrochimica Acta, 2019, 324, 134874.	5.2	68

#	Article	IF	CITATIONS
19	Facile preparation and characterization of poly(vinyl alcohol)-NaCl-glycerol supramolecular hydrogel electrolyte. European Polymer Journal, 2018, 106, 206-213.	5.4	67
20	Amphiphilic Gemini Iridium(III) Complex as a Mitochondria-Targeted Theranostic Agent for Tumor Imaging and Photodynamic Therapy. ACS Applied Materials & Interfaces, 2019, 11, 15276-15289.	8.0	66
21	Studies of the plasticizing effect of different hydrophilic inorganic salts on starch/poly (vinyl) Tj ETQq1 1 0.78431	4 rgBT /O ^v 7.5	verlock 10 T
22	An Antifreezing, Tough, Rehydratable, and Thermoplastic Poly(vinyl alcohol)/Sodium Alginate/Poly(ethylene glycol) Organohydrogel Electrolyte for Flexible Supercapacitors. ACS Sustainable Chemistry and Engineering, 2021, 9, 9833-9845.	6.7	54
23	A coumarin-based fluorescent probe for hypochlorite ion detection in environmental water samples and living cells. Talanta, 2019, 202, 303-307.	5.5	52
24	Highly flexible and adhesive poly(vinyl alcohol)/poly(acrylic amide-co-2-acrylamido-2-methylpropane) Tj ETQq0 0 0 Engineering Journal, 2021, 425, 131505.	rgBT /Ov 12.7	erlock 10 Tf 52
25	Preparation and characterization of quaternized poly(vinyl alcohol)/chitosan/MoS2 composite anion exchange membranes with high selectivity. Carbohydrate Polymers, 2018, 180, 96-103.	10.2	50
26	Stepwise synthesis of CoS ₂ –C@CoS ₂ yolk–shell nanocages with much enhanced electrocatalytic performances both in solar cells and hydrogen evolution reactions. Journal of Materials Chemistry A, 2018, 6, 12056-12065.	10.3	49
27	Facile preparation of N-O codoped hierarchically porous carbon from alginate particles for high performance supercapacitor. Journal of Colloid and Interface Science, 2020, 563, 414-425.	9.4	49
28	Cu-Ni-CoSex quaternary porous nanocubes as enhanced Pt-free electrocatalysts for highly efficient dye-sensitized solar cells and hydrogen evolution in alkaline medium. Chemical Engineering Journal, 2019, 357, 11-20.	12.7	47
29	Preparation and characterization of novel magnetic Fe3O4/chitosan/Al(OH)3 beads and its adsorption for fluoride. International Journal of Biological Macromolecules, 2018, 114, 256-262.	7.5	46
30	Cobalt iron selenide/sulfide porous nanocubes as high-performance electrocatalysts for efficient dye-sensitized solar cells. Journal of Power Sources, 2017, 369, 35-41.	7.8	45
31	Preparation and characterization of hybrid double network chitosan/poly(acrylic amide-acrylic acid) high toughness hydrogel through Al 3+ crosslinking. Carbohydrate Polymers, 2017, 173, 701-706.	10.2	43
32	Humidity-Responsive Gold Aerogel for Real-Time Monitoring of Human Breath. Langmuir, 2018, 34, 4908-4913.	3.5	39
33	Facile preparation of nitrogen-doped activated mesoporous carbon aerogel from chitosan for methyl orange adsorption from aqueous solution. Cellulose, 2019, 26, 4515-4527.	4.9	39
34	New efficient organic dyes employing indeno[1,2-b]indole as the donor moiety for dye-sensitized solar cells. Journal of Power Sources, 2016, 332, 103-110.	7.8	36
35	A facile preparation method for anti-freezing, tough, transparent, conductive and thermoplastic poly(vinyl alcohol)/sodium alginate/glycerol organohydrogel electrolyte. International Journal of Biological Macromolecules, 2020, 164, 2512-2523.	7.5	36
36	Facile preparation and characterization of super tough chitosan/poly(vinyl alcohol) hydrogel with low temperature resistance and anti-swelling property. International Journal of Biological Macromolecules, 2020, 142, 574-582.	7.5	34

#	Article	IF	CITATIONS
37	Ni–Fe–WSx polynary hollow nanoboxes as promising electrode catalysts for high-efficiency triiodide reduction in dye-sensitized solar cells. Journal of Alloys and Compounds, 2021, 851, 156899.	5.5	34
38	The effect of glycerol on properties of chitosan/poly(vinyl alcohol) films with AlCl 3 ·6H 2 O aqueous solution as the solvent for chitosan. Carbohydrate Polymers, 2016, 135, 191-198.	10.2	33
39	CoMoSx@Ni-CoMoSx double-shelled cage-in-cage hollow polyhedron as enhanced Pt-free catalytic material for high-efficiency dye-sensitized solar cell. Journal of Power Sources, 2019, 417, 21-28.	7.8	33
40	Efficient carbon dioxide electrolysis with metal nanoparticles loaded La0·75Sr0·25Cr0·5Mn0·5O3-δ cathodes. Journal of Power Sources, 2017, 363, 177-184.	7.8	31
41	Microporeâ€Forming Gelatin Methacryloyl (GelMA) Bioink Toolbox 2.0: Designable Tunability and Adaptability for 3D Bioprinting Applications. Small, 2022, 18, .	10.0	31
42	Template synthesis of cobalt molybdenum sulfide hollow nanoboxes as enhanced bifunctional Pt-free electrocatalysts for dye-sensitized solar cells and alkaline hydrogen evolution. Electrochimica Acta, 2018, 289, 448-458.	5.2	30
43	A covalent organic framework as a photocatalyst for atom transfer radical polymerization under white light irradiation. Polymer Chemistry, 2021, 12, 183-188.	3.9	30
44	Molecular p–n heterojunction-enhanced visible-light hydrogen evolution over a N-doped TiO ₂ photocatalyst. Catalysis Science and Technology, 2017, 7, 2039-2049.	4.1	27
45	Formation of CoTe2 embedded in nitrogen-doped carbon nanotubes-grafted polyhedrons with boosted electrocatalytic properties in dye-sensitized solar cells. Applied Surface Science, 2019, 476, 769-777.	6.1	27
46	Construction of Pt-free electrocatalysts based on hierarchical CoS2/N-doped C@Co-WS2 yolk-shell nano-polyhedrons for dye-sensitized solar cells. Electrochimica Acta, 2020, 340, 135949.	5.2	27
47	Construction of uniform Co–Sn–X (X = S, Se, Te) nanocages with enhanced photovoltaic and oxygen evolution properties <i>via</i> anion exchange reaction. Nanoscale, 2018, 10, 22012-22024.	5.6	26
48	Co-Ni-MoSx yolk-shell nanospheres as superior Pt-free electrode catalysts for highly efficient dye-sensitized solar cells. Journal of Power Sources, 2019, 412, 568-574.	7.8	26
49	A low-cost and environment friendly chitosan/aluminum hydroxide bead adsorbent for fluoride removal from aqueous solutions. Iranian Polymer Journal (English Edition), 2018, 27, 253-261.	2.4	24
50	Biofriendly and Regenerable Emotional Monitor from Interfacial Ultrathin 2D PDA/AuNPs Cross-linking Films. ACS Applied Materials & Interfaces, 2019, 11, 36259-36269.	8.0	24
51	Facile synthesis of MnO2 nanorods grown on porous carbon for supercapacitor with enhanced electrochemical performance. Journal of Colloid and Interface Science, 2019, 540, 466-475.	9.4	23
52	Facile Fabrication of Biochar/Al ₂ O ₃ Adsorbent and Its Application for Fluoride Removal from Aqueous Solution. Journal of Chemical & Engineering Data, 2019, 64, 83-89.	1.9	23
53	Visible Lightâ€Regulated Heterogeneous Catalytic PETâ€RAFT by High Crystallinity Covalent Organic Framework. Macromolecular Rapid Communications, 2021, 42, e2100384.	3.9	23
54	An adhesive, anti-freezing, and environment stable zwitterionic organohydrogel for flexible all-solid-state supercapacitor. Polymer, 2022, 254, 125109.	3.8	22

#	Article	IF	CITATIONS
55	MOF derived C/Co@C with a "one-way-valve―like graphitic carbon layer for selective semi-hydrogenation of aromatic alkynes. Carbon, 2020, 160, 64-70.	10.3	21
56	Indeno[1,2- b]indole-based organic dyes with different acceptor groups for dye-sensitized solar cells. Dyes and Pigments, 2017, 139, 274-282.	3.7	20
57	Effects of Câ€Related Dangling Bonds and Functional Groups on the Fluorescent and Electrochemiluminescent Properties of Carbonâ€Based Dots. Chemistry - A European Journal, 2018, 24, 4250-4254.	3.3	20
58	Distinctive Performance of Gemini Surfactant in the Preparation of Hierarchically Porous Carbons via High-Internal-Phase Emulsion Template. Langmuir, 2018, 34, 12100-12108.	3.5	20
59	Synthesis of CoS2/SnO2@MoS2 nanocube heterostructures for achieving enhanced electrocatalytic hydrogen evolution in acidic media. Inorganic Chemistry Frontiers, 2020, 7, 2660-2668.	6.0	20
60	Perovskite SrFeO3â^î^decorated with Ni nanoparticles for high temperature carbon dioxide electrolysis. International Journal of Hydrogen Energy, 2018, 43, 17040-17047.	7.1	19
61	Controlled synthesis of porous nanosheets-assembled peony-like cobalt nickel selenides for triiodide reduction in dye-sensitized solar cells. Journal of Alloys and Compounds, 2020, 818, 152817.	5.5	19
62	Syntheses, surface activities and aggregation morphologies of a series of novel itaconic acid based asymmetrical gemini surfactants. Journal of Molecular Liquids, 2019, 290, 111218.	4.9	18
63	A cyclometalated iridium(III) complex-based fluorescence probe for hypochlorite detection and its application by test strips. Analytical Biochemistry, 2019, 566, 27-31.	2.4	17
64	Multipath oxygen-mediated PET-RAFT polymerization by a conjugated organic polymer photocatalyst under red LED irradiation. Polymer Chemistry, 2021, 12, 6998-7004.	3.9	16
65	Oxygen-enriched hierarchical porous carbon supported Co-Ni nanoparticles for promising hybrid supercapacitors via one step pyrolysis of polymerized high internal phase emulsion. Journal of Alloys and Compounds, 2022, 907, 164481.	5.5	16
66	The Effect of glycerol on the crystalline, thermal, and tensile properties of CaCl ₂ â€doped starch/ <scp>PVA</scp> films. Polymer Composites, 2016, 37, 3191-3199.	4.6	15
67	Bimetallicâ€organic Frameworks CoMoâ€ZIFâ€67: An Efficient and Stable Catalyst for Selective Oxidation of Alkenes. ChemCatChem, 2021, 13, 416-424.	3.7	15
68	Durable and recyclable conjugated microporous polymer mediated controlled radical polymerization under white LED light irradiation. Polymer Chemistry, 2021, 12, 6714-6723.	3.9	15
69	Visible light-triggered PET-RAFT polymerization by heterogeneous 2D porphyrin-based COF photocatalyst under aqueous condition. European Polymer Journal, 2022, 173, 111306.	5.4	15
70	Tunable electrorheological characteristics and mechanism of a series of graphene-like molybdenum disulfide coated core–shell structured polystyrene microspheres. RSC Advances, 2016, 6, 26096-26103.	3.6	13
71	Binuclear molybdenum Schiff-base complex: An efficient catalyst for the epoxidation of alkenes. Molecular Catalysis, 2019, 475, 110498.	2.0	13
72	Amphiphilic gemini-iridium (III) complex for rapid and selective detection of picric acid in water and intracellular. Talanta, 2020, 208, 120372.	5.5	13

#	Article	IF	CITATIONS
73	Tuning the pore architectures of hierarchically porous carbons from high internal phase emulsion template by polyaniline-coated CNTs. Colloid and Polymer Science, 2020, 298, 179-191.	2.1	13
74	MoS2/Ni-CoSx porous nanocubes derived from Ni–Co prussian-blue analogs as enhanced Pt-free electrode catalysts for high-efficiency dye-sensitized solar cells. Journal of Power Sources, 2019, 440, 227121.	7.8	12
75	Coâ^'MOFâ€74@Cuâ^'MOFâ€74 Derived Bifunctional Coâ^'C@Cuâ^'C for Oneâ€Pot Production of 1, 4â€Dipheny 3â€Butadiene from Phenylacetylene. ChemCatChem, 2020, 12, 6241-6247.	ylâ€ 1 , 3.7	12
76	Preparation of N-doped porous carbons via high internal phase emulsion template. Progress in Natural Science: Materials International, 2021, 31, 270-278.	4.4	12
77	Photoinduced organocatalyzed controlled radical polymerization feasible over a wide range of wavelengths. Polymer Chemistry, 2022, 13, 527-535.	3.9	12
78	Surface patterning and modification of polyurethane biomaterials using silsesquioxane-gelatin additives for improved endothelial affinity. Science China Chemistry, 2014, 57, 596-604.	8.2	11
79	A water-soluble cyclometalated iridium(III) complex with fluorescent sensing capability for hypochlorite. Dyes and Pigments, 2019, 171, 107715.	3.7	11
80	A novel mitochondria-targeted phosphorescence probe for hypochlorite ions detection in living cells. Talanta, 2020, 209, 120516.	5.5	11
81	Fully-ï€ conjugated covalent organic frameworks as catalyst for photo-induced atom transfer radical polymerization with ppm-level copper concentration under LED irradiation. European Polymer Journal, 2021, 157, 110670.	5.4	11
82	Robust graphene/poly(vinyl alcohol) aerogel for highâ€flux and highâ€purity separation of waterâ€inâ€oil emulsion and its computational fluid dynamic simulation. AICHE Journal, 2022, 68, .	3.6	10
83	Tough and anti-fatigue double network gelatin/polyacrylamide/DMSO/Na2SO4 ionic conductive organohydrogel for flexible strain sensor. European Polymer Journal, 2022, 168, 111099.	5.4	10
84	Toughened elastomer/polyhedral oligomeric silsesquioxane (POSS)â€intercalated rectorite nanocomposites: Preparation, microstructure, and mechanical properties. Polymer Composites, 2017, 38, E443.	4.6	9
85	Heterogemini surfactant assisted synthesis of monodisperse icosahedral gold nanocrystals and their applications in electrochemical biosensing. RSC Advances, 2016, 6, 31301-31307.	3.6	8
86	Green synthesis of red-emission carbon based dots by microbial fermentation. New Journal of Chemistry, 2018, 42, 8591-8595.	2.8	8
87	Organocatalyzed controlled radical polymerization with alkyl bromide initiator via in situ halogen exchange under thermal condition. Polymer, 2020, 189, 122201.	3.8	7
88	Nitrogen, sulfur coâ€doped porous carbon via high internal phase emulsion template and its potential application as the electrode of highâ€performance supercapacitor. Journal of Applied Polymer Science, 2022, 139, .	2.6	7
89	Phosphorescent iridium(III) complex for efficient sensing of hypochlorite and imaging in living cells. Analytical Biochemistry, 2020, 592, 113573.	2.4	6
90	<scp>Imineâ€based</scp> covalent organic framework as photocatalyst for <scp>visibleâ€lightâ€induced</scp> atom transfer radical polymerization. Journal of Polymer Science, 2021, 59, 2036-2044.	3.8	6

#	Article	IF	CITATIONS
91	A quaternized poly(vinyl alcohol)/chitosan composite alkaline polymer electrolyte: preparation and characterization of the membrane. Iranian Polymer Journal (English Edition), 2017, 26, 531-539.	2.4	5
92	Synergism Effect of Surfactant and Inorganic Salt on the Properties of Starch/Poly(Vinyl Alcohol) Film. Starch/Staerke, 2018, 70, 1700146.	2.1	5
93	Phaseâ€Controlled Cobalt Phosphide Nanoparticles Coupled with N, P, S Coâ€Doped Hollow Carbon Polyhedrons as Efficient Catalysts for Both Alkaline and Acidic Hydrogen Evolution. Energy Technology, 2019, 7, 1800757.	3.8	5
94	Efficient Persistent Luminescence Tuning Using a Cyclodextrin Inclusion Complex as Efficient Light Conversion Materials. ACS Omega, 2021, 6, 25585-25593.	3.5	4
95	A sensitive "Switch-on―phosphorescent probe for ferrous iron quantification in drug and In vitro imaging of living cells. Talanta, 2020, 217, 121097.	5.5	3
96	Remarkable binuclear Schiffâ€based complex catalyze the epoxidation of alkenes: effects of substituent group. Applied Organometallic Chemistry, 2020, 34, e5608.	3.5	3
97	Temperature-sensitive poly(N-isopropylacrylamide)–reduced graphene oxide/polysulfone as smart separation membrane: structure and performance. Iranian Polymer Journal (English Edition), 2018, 27, 951-963.	2.4	2
98	Preparation of fluorescent polystyrene nanoparticles mediated by a multi-functional amphiphilic iridium complex under visible light irradiation in aqueous solution. Polymer Chemistry, 2020, 11, 795-799.	3.9	2
99	Asymmetrical Gemini Surfactants Directed Synthesis Of Hierarchical ZSMâ€5 Zeolites and Their Immobilization of Molybdenum Complex for the Catalytic Epoxidation of Alkenes. ChemCatChem, 2021, 13, 4442.	3.7	2
100	Influences of nonsolvent on the morphologies and electrochemical properties of carbon nanofibres from electrospun polyacrylonitrile nanofibres. Bulletin of Materials Science, 2018, 41, 1.	1.7	1
101	Epoxy-based composites with enhanced thermal properties through collective effect of different particle size fillers. Polymers and Polymer Composites, 2022, 30, 096739112211066.	1.9	1
102	Synthesis of porous silica materials with tunable morphologies and nanopore sizes using heterogemini surfactants. Micro and Nano Letters, 2018, 13, 725-727.	1.3	0